



## ORIGINAL ARTICLE

# Technetium-labeled danofloxacin complex as a model for infection imaging



Moustapha Eid Moustapha <sup>a,\*</sup>, Hoda A. Shweeta <sup>b,c</sup>, Mohamed A. Motaleb <sup>c</sup>

<sup>a</sup> Chemistry Department, Prince Sattam bin Abdulaziz University, AlKharj 11942, Saudi Arabia

<sup>b</sup> College of Pharmacy, Umm Al-Qura University, Makkah, Saudi Arabia

<sup>c</sup> Labeled Compound Department, Hot Lab. Center, Atomic Energy Authority, P.O. Box 13759, Cairo, Egypt

Received 21 April 2014; accepted 9 October 2014

Available online 16 October 2014

## KEYWORDS

Danofloxacin;  
Labeling;  
Technetium;  
Inflammation;  
Infection;  
Diagnosis

**Abstract** Danofloxacin, a fluoroquinolone derivative antibiotic, was synthesized, successfully labeled with technetium-99m and formulated for the development of a potential diagnostic imaging agent of the bacterial infection and inflammation with higher efficiency than that of the commercially available <sup>99m</sup>Tc-ciprofloxacin. Factors affecting the labeling yield were optimized. The radiolabeled antibiotic was subjected to preclinical assessments such as purity, stability, and pharmacokinetic investigations in animals. The biodistribution studies indicated that the uptake of <sup>99m</sup>Tc-danofloxacin was high in the infectious lesion (T/NT = 7.2 ± 0.1) at 2 h post injection. The abscess to normal ratio indicated that the danofloxacin tracer can be used for infection diagnosis. The radiolabeled compound was cleared quickly from most of the body organs. The results displayed that <sup>99m</sup>Tc-danofloxacin could not differentiate between infection and sterile inflammation. © 2014 The Authors. Production and hosting by Elsevier B.V. on behalf of King Saud University. This is an open access article under the CC BY-NC-ND license (<http://creativecommons.org/licenses/by-nc-nd/3.0/>).

## 1. Introduction

The rate of morbidity and mortality could be reduced if infection and inflammation can be clinically diagnosed and treated with appropriate drugs at early stage (Qaiser et al., 2010). Modern imaging techniques and procedures for diagnosis of infection such as Magnetic Resonance Imaging (MRI),

Computer Tomography (CT), X-ray and Ultrasonography (US) are commercially available and have been used for the detection of infection. These tools are not the appropriate methods for the diagnosis and localization of infection at early stages because they cannot reveal the change in the morphology of tissues following the abscess formation (Motaleb, 2007; Lucignani, 2007 and Gemmel et al., 2009). The role of several Nuclear Medicine Scintigraphy (NMS) techniques in early diagnosis or discrimination between infection and inflammation is clinically vital for the appropriate management of patients with microbial infectious or inflammatory diseases (Saha, 2004; Lupetti et al., 2007 and Langer et al., 2005). The introduction of a number of radiopharmaceuticals in Nuclear Medicine used as infection imaging agents was reported including radiolabeled leukocytes and <sup>67</sup>Ga-citrate (Palestro, 2007 and Yapar et al., 2001). Due to the

\* Corresponding author.

E-mail addresses: [memoustapha@gmail.com](mailto:memoustapha@gmail.com), [m.moustapha@sau.edu.sa](mailto:m.moustapha@sau.edu.sa) (M. Eid Moustapha).

Peer review under responsibility of King Saud University.



Production and hosting by Elsevier

<http://dx.doi.org/10.1016/j.arabjc.2014.10.017>

1878-5352 © 2014 The Authors. Production and hosting by Elsevier B.V. on behalf of King Saud University.

This is an open access article under the CC BY-NC-ND license (<http://creativecommons.org/licenses/by-nc-nd/3.0/>).

inconveniences and limitations of the conventional infection imaging agents such as time-consuming preparation, the lack of specificity, sensitivity and high radiation burden, the development of new radiopharmaceuticals for infection imaging represents a major challenge for nuclear medicine and molecular imaging (Singh et al., 2003; Martin-Comin et al., 2004; Sakr et al., 2013 and Moustapha et al., 2011).

Several radiolabeled antibiotics have been synthesized and are potentially promising kits for the diagnostic imaging of infective lesions (Singh et al., 2010; Esposito et al., 2009; Asikoglu et al., 2000 and Brunton and Parker, 2008). The ideal radiolabeled antibiotic agents should highly localize in the infectious foci, where they are frequently taken up, metabolized and display fast clearance from the body. Quinolones (ceftriaxone, norfloxacin, sitafloxacin, enrofloxacin, ciprofloxacin, lomefloxacin, sparfloxacin, difloxacin, levofloxacin, pefloxacin, moxifloxacin and ceftizoxime) are broad spectrum antibiotics that are widely used as the major treatment of serious bacterial infections (Hazari et al., 2009; Nieto et al., 2005; Starovoitova et al., 2014; Anderson and Kodukula, 2014 and Ziessman et al., 2014). Ciprofloxacin labeled with  $^{99m}\text{Tc}$  is considered as one of the most important radiopharmaceuticals commercially available for infection imaging (Chattopadhyay et al., 2010; Dumarey et al., 2002; Gemmel et al., 2004 and IAEA, 2008). However, data of biodistribution in experimental animals and in human studies reported that the specificity of  $^{99m}\text{Tc}$ -ciprofloxacin for infection is contradictory (Yapar et al., 2001; Sarda et al., 2002, 2003; Larikka et al., 2002a,b; Siaens et al., 2004; Pauwels et al., 2001).  $^{99m}\text{Tc}$ -ciprofloxacin preparation has many disadvantages which are discussed in detail in the literatures (Signore et al., 2008; Siaens et al., 2004; Zolle, 2007 and Britton et al., 1997).

Danofloxacin is a fluoroquinolone derivative with broad spectrum antibacterial activity toward both Gram positive and Gram negative pathogenic bacteria. The structure of danofloxacin is shown in Fig. 1 (USP/NF, 2008). The purpose of the present study was to establish a simple and efficient method for synthesis and labeling danofloxacin with  $^{99m}\text{Tc}$  as a potential infection imaging agent to reveal the sites of bacterial infections *in vivo*. The formulation of the labeled drug will have to be optimized based on preclinical assessments with respect to *in vitro* and *in vivo* stability, radiochemical purity and pharmacokinetic studies in animals.

## 2. Materials and methods

Danofloxacin ( $\text{C}_{19}\text{H}_{20}\text{FN}_3\text{O}_3$ ; M.wt. = 357.37 g/mol) was purchased from Sigma–Aldrich, USA. Whatman No. 1 paper chromatography (PC) was obtained from Whatman International Ltd., Maidstone, UK. Technetium-99 m ( $t_{1/2} = 6\text{ h}$ ) was eluted as  $^{99m}\text{TcO}_4^-$  from  $^{99}\text{Mo}/^{99m}\text{Tc}$  generator, Gentech,

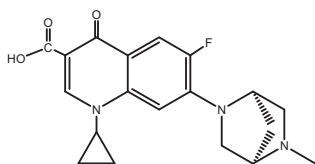


Figure 1 Chemical structure of danofloxacin.

Turkey. Measurement of radioactivity was performed in a Well-type NaI(Tl) gamma( $\gamma$ )counter. All reagents and solvents used were of analytical reagent grade and used without further purification. Deionized water was used in all experiments.

### 2.1. Labeling procedure

$^{99m}\text{Tc}$ -danofloxacin was synthesized by direct reaction of danofloxacin with technetium-99m. An accurate amount of 1 mg danofloxacin was transferred to an evacuated penicillin vial. A freshly prepared deoxygenated aqueous solution containing exactly 50  $\mu\text{g}$  of  $\text{SnCl}_2 \cdot 2\text{H}_2\text{O}$  was added and the pH of the preparation was adjusted to 11 using phosphate buffer. One ml of  $^{99m}\text{Tc}$  eluate containing 400 MBq was introduced to the above reaction mixture, mixed and left to react at room temperature (25  $^\circ\text{C}$ ) under sterile conditions for 30 min before estimating the yield of the produced complex. The reaction conditions affecting the radiolabeling yield such as stannous chloride amount (25–200  $\mu\text{g}$ ), danofloxacin amount (0.5–2.5 mg), pH of the reaction mixture (5–12) and the reaction time (1–480 min) were investigated and optimized in order to maximize the labeling efficiency. Paper chromatography (PC) and high performance liquid chromatography (HPLC) were used to assess the radiochemical purity.

### 2.2. Analysis

Radiochemical purity of a radiopharmaceutical product is the proportion of the total radioactivity in the desired radiochemical form. Different analytical methods including PC and HPLC are used to assess the radiochemical impurities present in the reaction mixture with the  $^{99m}\text{Tc}$ -labeled complex. Radiochemical impurities are hydrolyzed  $^{99m}\text{Tc}$  and free  $^{99m}\text{TcO}_4^-$ . Radiochemical purity of  $^{99m}\text{Tc}$ -danofloxacin was determined by the ascending paper chromatographic technique using strips of Whatman No. 1 paper chromatography (PC). Two strips (1 cm width, 13 cm length) were marked 2 cm from the bottom edge of the strip and lined into segments 1 cm each up to 13 cm. A spot of 1–2  $\mu\text{l}$  of the filtered reaction mixture containing the labeled complex was applied above the lower edge and allowed to evaporate spontaneously. Then one strip was placed in a closed jar and developed with acetone to determine the percentage of free pertechnetate ( $^{99m}\text{TcO}_4^-$ ) while the other strip was developed with a mixture of ethanol: water: ammonia (2:5:1) to detect the percentage of reduced hydrolyzed technetium-99m. After complete development the strips were removed, dried and cut into segments of 1 cm each. The radioactivity was counted using a Well-type  $\gamma$ -scintillation detector.

The radiochemical purity was further confirmed by HPLC. Chromatographic analysis was performed by injection of 10  $\mu\text{l}$  of purified reaction mixture containing  $^{99m}\text{Tc}$ -danofloxacin at the optimum conditions into a reversed-phase column (Lichrosorb RP C-18, 4 mm  $\times$  250 mm; 5  $\mu\text{m}$ ) coupled to a UV detector (SPD-6A) set at 320 nm and eluted with a mobile phase consisting of a mixture of 10% ethanol in 0.2 M phosphate buffer at pH 7.2. The filtered mobile phase was degassed prior to use and the flow rate was adjusted to 0.5 ml/min. (Moustapha et al., 2013; Al-wabli et al., 2011). Radioactivity measurements in the HPLC eluates were detected by NaI(Tl) scintillation detector coupled to a single channel analyzer.

### 2.3. Stability of $^{99m}\text{Tc}$ -danofloxacin in serum

Stability of the labeled complex was determined by mixing 1.8 ml of the normal serum and 0.2 ml of  $^{99m}\text{Tc}$ -danofloxacin at 37 °C for 24 h. During the *in vitro* incubation period, aliquots of 0.2 ml each were withdrawn at different time intervals for up to 24 h and analyzed using instant thin layer chromatography (ITLC) and HPLC to determine the percentage of the formed  $^{99m}\text{Tc}$ -complex, reduced hydrolyzed technetium and free pertechnetate.

### 2.4. Induction of inflammation in mice

Induction of infectious foci was evaluated by the method reported by Al-wabli in which a single clinical isolation of *Staphylococcus aureus* from biological samples was used to produce focal infection (Al-wabli et al., 2011). Individual colonies were diluted in order to obtain turbid suspension. Groups of three mice were intramuscularly injected with 200  $\mu\text{l}$  of the suspension in the left lateral thigh muscle. Then, the mice were left for 24 h to get a gross swelling in the infected thigh. On the other hand, non-infected inflammation (sterile inflammation) was induced by injecting 200  $\mu\text{l}$  of turpentine oil sterilized by autoclaving at 121 °C for 20 min., intramuscularly administered in the left lateral thigh muscle of the mice. Two days later, swelling appeared (Mostafa et al., 2010; Asikoglu et al., 2000). Similarly, induction of heat killed non-infected inflammation was induced by injecting 200  $\mu\text{l}$  of heat killed *S. aureus* (Larikka et al., 2002a,b; Oyen et al., 2001 and Kaul et al., 2013).

### 2.5. Biodistribution studies

*In vivo* experiments were conducted in accordance with the guidelines of the Egyptian Atomic Energy Authority and the animal ethics committee. Prior to the biodistribution experiment, normal Albino mice were housed in groups ( $n = 5$ ) for different intervals of time under normal conditions. Animals were injected intravenously in the tail vein with 100  $\mu\text{l}$  of  $^{99m}\text{Tc}$ -danofloxacin (4 MBq). Mice were sacrificed by cervical dislocation at 2, 4 and 24 h after administration of  $^{99m}\text{Tc}$ -danofloxacin. A blood sample was obtained by heart puncture. Both target and non-target thighs were dissected and counted. After dissection, the organs were removed, washed with saline, collected in plastic tubes and weighed. The radioactivity of each sample and the background was counted in a Well-type NaI(Tl) gamma spectrometer. Results were reported as percent-injected dose per gram organ (% ID/g organ  $\pm$  SD) in a population of five mice for each time point. Statistics are evaluated with the Student's *t* test and all results are given as mean  $\pm$  SEM.

## 3. Results and discussion

Radiochemical purity and *in vitro* stability of  $^{99m}\text{Tc}$ -danofloxacin complex were assessed by PC and further confirmed by HPLC. Acetone was used as the developing solvent to determine free  $^{99m}\text{TcO}_4^-$ , which moved with the solvent front ( $R_f = 1$ ), while  $^{99m}\text{Tc}$ -danofloxacin and reduced hydrolyzed technetium remained at the origin ( $R_f = 0$ ). Reduced

hydrolyzed technetium was detected using a mixture of ethanol: water: ammonium hydroxide (2:5:1 v/v) as the developing solvent, where it remains at the origin ( $R_f = 0$ ) while other species migrate with the solvent front ( $R_f = 1$ ). The undesirable radiochemical species such as the free and hydrolyzed fractions must be removed or reduced to a minimum level in order not to change the biodistribution of the labeled compound resulting in a significant interference with the diagnostic image. The radiochemical purity was determined by subtracting the sum of the percent of reduced hydrolyzed technetium and free pertechnetate from 100%. The radiochemical yield is the mean value of three experiments. The radiochemical purity was further confirmed by HPLC analysis, where the retention time of free  $^{99m}\text{TcO}_4^-$  and  $^{99m}\text{Tc}$ -danofloxacin was 5 and 18.9 min, respectively as illustrated in the radiochromatogram (Fig. 2). In other words, quality control and purification of  $^{99m}\text{Tc}$ -danofloxacin were performed by HPLC. It was able to separate the labeled compound from the unlabeled compound and the free pertechnetate. Factors affecting the labeling yield will be discussed in detail.

### 3.1. Effect of danofloxacin amount

Danofloxacin was labeled with technetium-99m using the direct technique in which the reduced technetium-99m reacted with danofloxacin to form the labeled chelate. The influence of labeling yield on the amount of danofloxacin actually present in the reaction mixture is illustrated in Fig. 3. The reaction was performed at different danofloxacin amounts (0.5–2.5 mg). Exactly 1 mg was the optimum ligand amount required to obtain maximum radiochemical yield,  $90 \pm 2\%$ . Below this value, the ligand amount was insufficient to complex all the reduced technetium-99m toward the formation of  $^{99m}\text{Tc}$ -danofloxacin, as a result the reduced hydrolyzed technetium was 53% at 0.5 mg of danofloxacin. At ligand amount above 1 mg, the yield slightly decreased but did not change substantially and remained stable.

### 3.2. Effect of stannous chloride amount

Stannous chloride ( $\text{SnCl}_2 \cdot 2\text{H}_2\text{O}$ ) is the most commonly used reducing agent for the reduction of the pertechnetate ion ( $^{99m}\text{TcO}_4^-$ ), having the oxidation state (VII) to lower oxidation state, which favors its chelation by danofloxacin. The labeling process was affected by the amount of stannous chloride present in the labeling reaction as demonstrated in Fig. 4. The labeling yield of  $^{99m}\text{Tc}$ -danofloxacin was 73% after adding 25  $\mu\text{g}$   $\text{SnCl}_2 \cdot 2\text{H}_2\text{O}$  to the reaction mixture. This may be attributed to incomplete reduction of  $^{99m}\text{TcO}_4^-$  and hence unreliable yield of the complex due to the presence of free  $^{99m}\text{TcO}_4^-$  (13%). The labeling yield was maximized significantly (90%) by increasing the amount of  $\text{SnCl}_2 \cdot 2\text{H}_2\text{O}$  from 25 to 50  $\mu\text{g}$ . Increasing the amount of  $\text{SnCl}_2 \cdot 2\text{H}_2\text{O}$  to 200  $\mu\text{g}$  leads to a substantial decrease in the labeling yield (48%) due to the formation of tin colloids (52%). Increasing the amount of  $\text{SnCl}_2 \cdot 2\text{H}_2\text{O}$  above the optimum value (50  $\mu\text{g}$ ) leads to competition of danofloxacin for the reduced  $^{99m}\text{Tc}$ . The formation of the undesired tin colloid may be explained according to the fact that most of the ligand molecules were consumed in the formation of complex, hence the reduced pertechnetate may form  $^{99m}\text{Tc}$ -Sn-colloid and other Sn-complexes in the absence

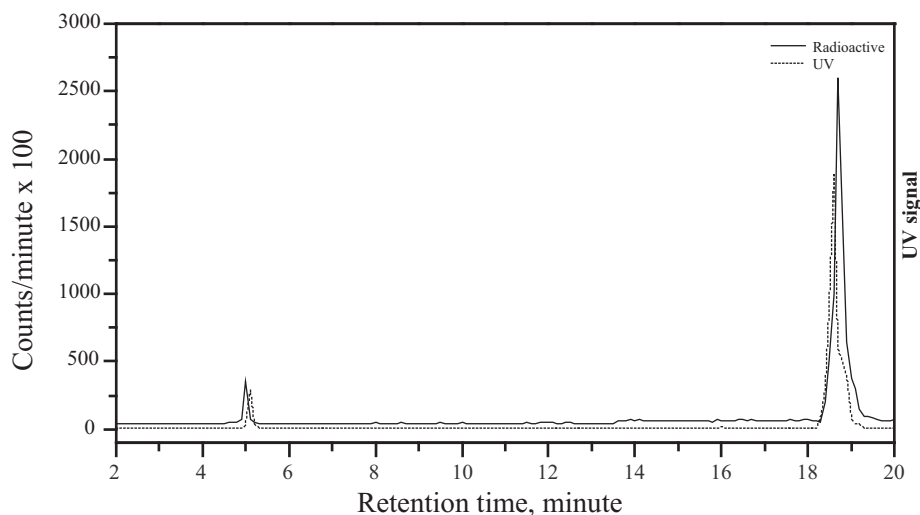


Figure 2 HPLC radiochromatogram of  $^{99m}\text{Tc}$  danofloxacin.

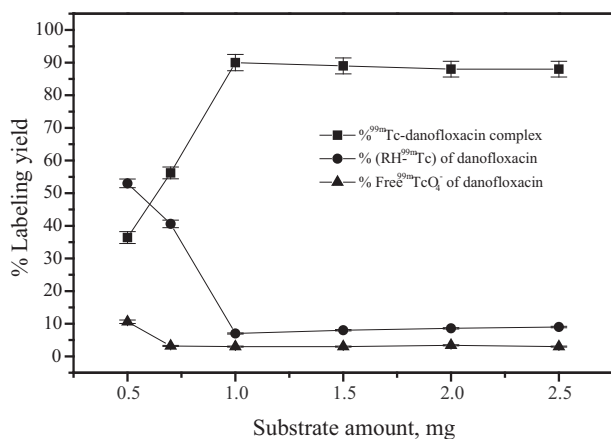


Figure 3 Effect of substrate content on the percent labeling yield of  $^{99m}\text{Tc}$ -danofloxacin complex.

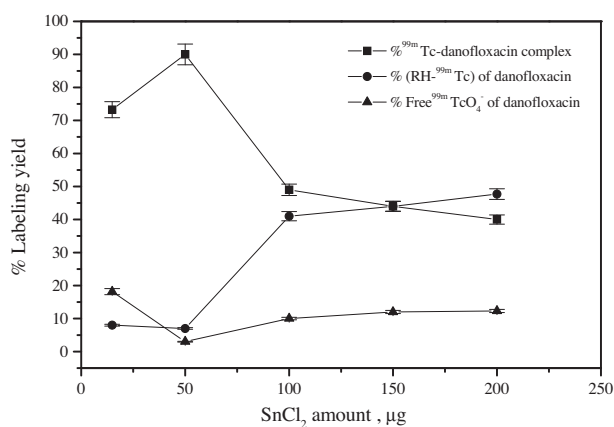


Figure 4 Effect of  $\text{SnCl}_2 \cdot 2\text{H}_2\text{O}$  content on the percent labeling yield of  $^{99m}\text{Tc}$ -danofloxacin complex.

of the ligand. On the other hand, the raise of stannous chloride amount leads to the formation of stannous hydroxide colloid  $\text{Sn}(\text{OH})_3^-$  impurities in alkaline medium, which in turn compete with the chelation process of danofloxacin and thus

reduces the yield of the  $^{99m}\text{Tc}$  chelate (Jurisson and Lydon, 1999; Saha, 2004).

### 3.3. Effect of pH

The labeling yield was affected by changes in pH of the reaction mixture as illustrated in Fig. 5. At pH 11 the labeling efficiency of  $^{99m}\text{Tc}$ -danofloxacin was equal to  $90 \pm 2\%$ . The maximum yield may be due to the deprotonation of the danofloxacin at high pH values, which increased the stability of  $^{99m}\text{TcO}(\text{V})$ -danofloxacin complex. At alkaline pH values, the presence of high  $\text{OH}^-$  concentration in the reaction mixture may lead to the partial hydrolysis of the formed complex and incomplete reduction of  $^{99m}\text{Tc}$  to the desired oxidation state, and hence produce an unreliable yield of the  $^{99m}\text{Tc}$ -danofloxacin besides the unreacted  $^{99m}\text{TcO}_4^-$ .

### 3.4. Effect of in vitro stability of $^{99m}\text{Tc}$ -danofloxacin and reaction time

Fig. 6 indicates that the rate of formation of  $^{99m}\text{Tc}$ -danofloxacin complex was strongly dependent on reaction time. The labeling

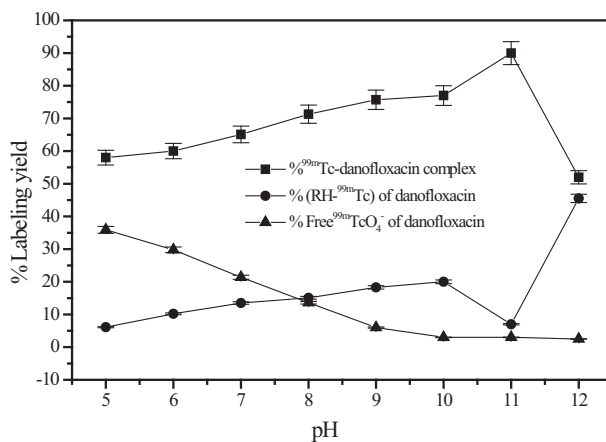
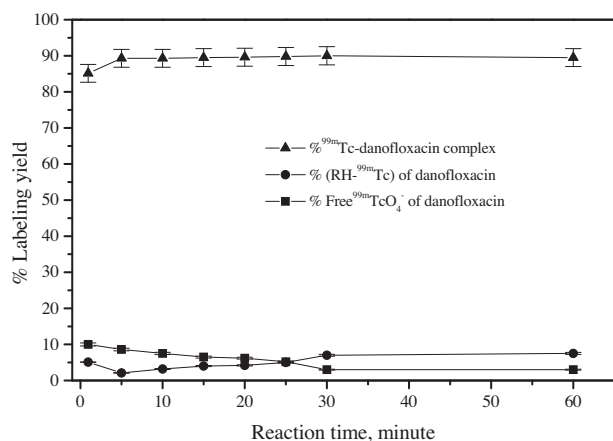
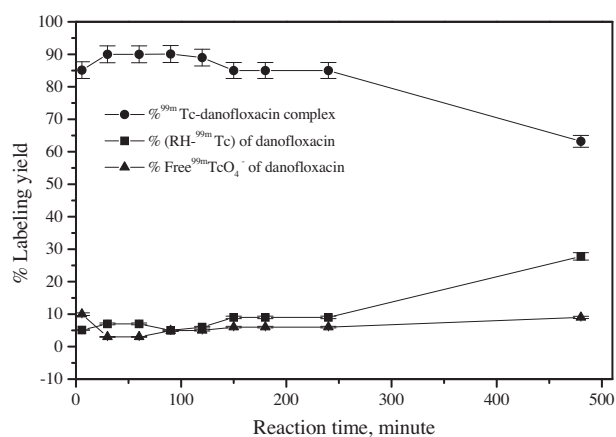


Figure 5 Effect of pH value of the reaction mixture on the percent labeling yield of  $^{99m}\text{Tc}$ -danofloxacin complex.



**Figure 6** Effect of reaction time on  $^{99m}\text{Tc}$ -danofloxacin complex.



**Figure 7** Stability test for  $^{99m}\text{Tc}$ -danofloxacin.

yield increased from 85% to 90% when increasing the reaction time from 1 to 30 min. *In vitro* stability of  $^{99m}\text{Tc}$ -danofloxacin was investigated over time. Fig. 7 indicates that the labeled fluo-

roquinolone derivative was stable for up to 120 min after labeling. The stability was found to be time-dependent with respect to some factors such as temperature, light and radiolysis, which may lead to the decomposition of the compound and limited its availability prior to injection.

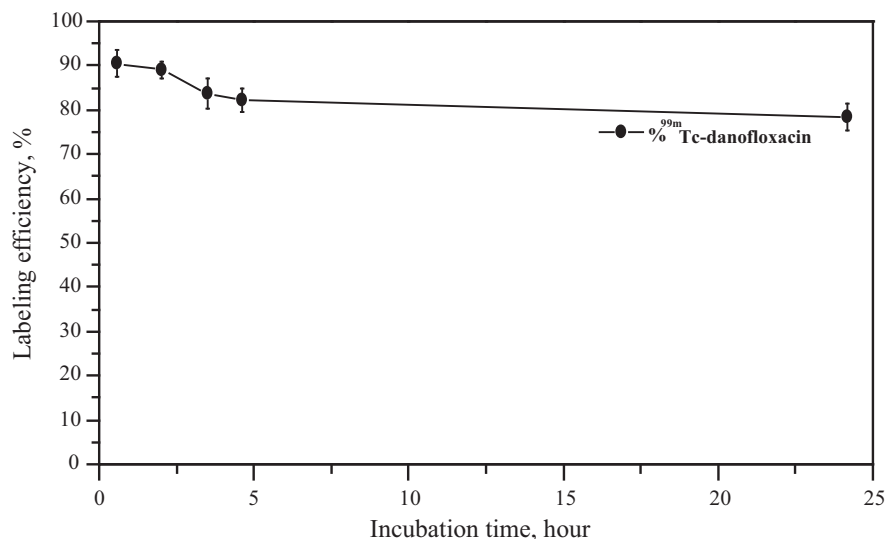
### 3.5. Stability test

As shown in Fig. 8, incubation of  $^{99m}\text{Tc}$ -danofloxacin in normal serum for 24 h at 37 °C resulted in a small release of radioactivity ( $13 \pm 1\%$ ,  $n = 5$  experiments) from the  $^{99m}\text{Tc}$ -complex, as determined by HPLC and ITLC. Therefore, the stability of the labeled complex indicated its suitability for *in vivo* application over time.

### 3.6. Biodistribution

Biodistribution data of the mice infected with living, heat killed *S. aureus* and turpentine oil are shown in Table 1. The uptake of  $^{99m}\text{Tc}$ -danofloxacin was significantly low in heat killed *S. aureus* and turpentine oil infected animals (aseptic inflammation) as compared to infected animals with living bacteria (abscess). These data indicated high uptake in the inflamed areas within 2 h after intravenous administration of the labeled compound via the tail vein. A rapid distribution of radioactivity was observed throughout the body. The uptake of  $^{99m}\text{Tc}$ -danofloxacin in different organs demonstrated that the injected tracer was cleared from the blood stream 24 h post injection. The major remaining activity of the tracer was found in the kidneys ( $6.6 \pm 0.4\%$  ID) and urine ( $30 \pm 3\%$  ID). In contrast, a significant level of radioactivity was retained in the liver ( $5.4 \pm 0.3\%$  ID). Elimination of  $^{99m}\text{Tc}$ -danofloxacin appeared to be by both renal and hepatic routes.

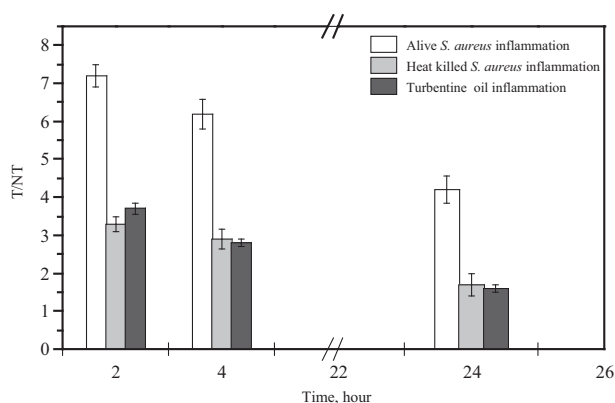
Mice with infectious lesions injected with  $^{99m}\text{Tc}$ -fluoroquinolone revealed a mean abscess-to-muscle (target to non-target, T/NT) ratio equal to  $7.2 \pm 0.1$  after 2 h post injection, which express higher uptake in infected tissue than the commercially available  $^{99m}\text{Tc}$ -ciprofloxacin (T/NT =  $3.8 \pm 0.8$ ) (Rien et al., 2004) as shown in Fig 9.



**Figure 8** *In vitro* stability of  $^{99m}\text{Tc}$ -danofloxacin in normal serum.

**Table 1** Biodistribution of  $^{99m}\text{Tc}$ -danofloxacin in *Staphylococcus aureus*, heat killed *Staphylococcus aureus* and turpentine oil inflamed mice at different time intervals.

Organs and body fluids	% Injected dose/organs at different time intervals (h)								
	<i>S. aureus</i>			Heat killed <i>S. aureus</i>			Turpentine oil		
	2	4	24	2	4	24	2	4	24
Inflamed muscle	1.8 ± 0.2	1.3 ± 0.1	0.8 ± 0.1	0.97 ± 0.1	0.75 ± 0.2	0.25 ± 0.1	1.1 ± 0.0	0.69 ± 0.2	0.21 ± 0.1
Control muscle	0.25 ± 0.1	0.21 ± 0.2	0.19 ± 0.0	0.29 ± 0.0	0.26 ± 0.1	0.15 ± 0.0	0.30 ± 0.0	0.25 ± 0.0	0.13 ± 0.0
Liver	17.1 ± 3.2	12.9 ± 2.0	5.4 ± 0.3	17.6 ± 2.4	12.2 ± 2.2	4.9 ± 0.5	17.5 ± 3.0	13.2 ± 2.2	6.1 ± 0.6
Urine	18.5 ± 3.5	24.9 ± 4.2	29.9 ± 3.1	17.1 ± 1.3	24.3 ± 1.1	29.4 ± 2.7	18.0 ± 0.9	25.4 ± 1.8	28.8 ± 2.4
Kidneys	11.2 ± 1.2	10.7 ± 1.3	6.6 ± 0.4	10.9 ± 1.3	10.2 ± 2.3	5.5 ± 0.7	11.3 ± 2.5	10.2 ± 1.2	6.9 ± 0.3
Blood	5.3 ± 0.4	3.1 ± 0.2	1.00 ± 0.0	6.10 ± 0.2	4.0 ± 0.2	1.0 ± 0.1	5.5 ± 0.2	4.3 ± 0.2	1.0 ± 0.0
Heart	0.3 ± 0.1	0.1 ± 0.0	0.09 ± 0.0	0.3 ± 0.09	0.1 ± 0.0	0.1 ± 0.0	0.4 ± 0.08	0.2 ± 0.0	0.1 ± 0.0
Lung	1.2 ± 0.2	0.2 ± 0.0	0.1 ± 0.0	1.1 ± 0.09	0.2 ± 0.0	0.1 ± 0.0	1.3 ± 0.09	0.4 ± 0.1	0.2 ± 0.0
Intestine and stomach	19.9 ± 2.5	3.90 ± 0.5	2.10 ± 0.3	19.1 ± 3.4	4.7 ± 0.4	2.2 ± 0.7	18.9 ± 1.9	4.7 ± 0.8	2.4 ± 0.4
Spleen	2.10 ± 0.1	1.00 ± 0.2	0.3 ± 0.1	2.1 ± 0.3	1.1 ± 0.0	0.5 ± 0.1	2.0 ± 0.1	1.3 ± 0.0	0.3 ± 0.0
Bone	0.90 ± 0.0	0.40 ± 0.1	0.10 ± 0.0	1.0 ± 0.0	0.49 ± 0.1	0.1 ± 0.0	1.1 ± 0.2	0.5 ± 0.1	0.1 ± 0.0

**Figure 9** The ratio of target muscle (T) to non-target muscle (NT) of  $^{99m}\text{Tc}$ -danofloxacin in different inflammation models at different post injection times.

#### 4. Conclusions

This study characterized the *in vitro* and *in vivo* conditions necessary for designing  $^{99m}\text{Tc}$ -danofloxacin complex as a potentially useful radiopharmaceutical for diagnosing bacterial infection. Danofloxacin was successfully labeled with technetium-99m by the direct labeling method at room temperature with a labeling yield of 90% using stannous chloride as a reducing agent. The excellent localization of the tracer in the induced foci of inflammation expressed the effectiveness of this complex for targeting infectious lesions, which was higher than the commercially available  $^{99m}\text{Tc}$ -ciprofloxacin.

#### Acknowledgement

This project was supported by the Deanship of Scientific Research at Prince Sattam Bin Abdulaziz University under the research project #.2015/01/5126.

#### References

Al-wabli, R.I., Motaleb, M.A., Kadi, A.A., Al-rashood, K.A., Zagahry, W.A., 2011. Labeling and biodistribution of  $^{99m}\text{Tc}$ -7-

- bromo-1,4-dihydro-4-oxo-quinolin-3-carboxylic acid complex. *J. Radioanal. Nucl. Chem.* 290, 507–513.
- Anderson, D.C., Kodukula, K., 2014. Biomarkers in pharmacology and drug discovery. *Biochem. Pharmacol.* 87, 172–188.
- Asikoglu, M., Yurt, F., Cagliyan, O., Unak, P., Ozkiliç, H., 2000. Detecting inflammation with  $^{131}\text{I}$ -labeled ornidazole. *Appl. Radiat. Isot.* 53, 411–413.
- Britton, K.E., Vinjamuri, S., Hall, A.V., Solanki, K., Siraj, Q.H., Bomanji, J., 1997. Clinical evaluation of technetium-99m infection for the localization of bacterial infection. *Eur. J. Nucl. Med.* 24, 553–556.
- Brunton, L.L., Parker, K.L., 2008. *Goodman & Gilman's Manual of Pharmacology and Therapeutics*. McGraw-Hill, New York.
- Chattopadhyay, S., Das, S.S., Chandra, S., De, K., Mishra, M., Sarkar, B.R., Sinha, S., Ganguly, S., 2010. Synthesis and evaluation of  $^{99m}\text{Tc}$ -moxifloxacin, a potential infection specific imaging agent. *Appl. Radiat. Isot.* 68, 314–316.
- Dumarey, N., Blocklet, D., Appelboom, T., Tant, L., Schoutens, A., 2002. Infection is not specific for bacterial osteo-articular infective pathology. *Eur. J. Nucl. Med.* 29, 530–535.
- Esposito, S., Leone, S., Bassetti, M., Borre, S., Leoncini, F., Meani, E., Venditti, M., Mazzotta, F., 2009. Italian guidelines for the diagnosis and infectious disease management of osteomyelitis and prosthetic joint infections in adults. *Infection* 37, 478–496.
- Gemmel, F., Winter, F., DeVanLaere, K., Vogelaers, D., Uyttendaele, D., Dierckx, R.A., 2004.  $^{99m}\text{Tc}$  ciprofloxacin imaging for the diagnosis of infection in the postoperative spine. *Nucl. Med. Commun.* 25, 277–283.
- Gemmel, F., Dumarey, N., Welling, M., 2009. Future diagnostic agents. *Semin. Nucl. Med.* 39, 11–26.
- Hazari, P.P., Chuttani, K., Nitin, K., Rashi, M., Sharma, R., Singh, B., 2009. Synthesis and biological evaluation of isonicotinic acid hydrazide conjugated with diethylenetriamine penta acetic acid for infection imaging. *Open Nucl. Med. J.* 1, 33–42.
- IAEA, 2008. Technical Reports Series No. 466. *Technetium-99m Radiopharmaceuticals: Manufacture of Kits*. International Atomic Energy Agency, Vienna.
- Jurisson, S.S., Lydon, J.D., 1999. Potential technetium small molecule radiopharmaceuticals. *Chem. Rev.* 99, 2205–2218.
- Kaul, A., Hazari, P.P., Rawat, H., Singh, B., Kalawat, T.C., Sharma, S., Anil Babbar, A.K., Mishra, A.K., 2013. Preliminary evaluation of technetium-99m-labeled ceftriaxone: infection imaging agent for the clinical diagnosis of orthopedic infection. *Int. J. Infect. Dis.* 17, 263–270.

- Langer, O., Brunner, M., Zeitlinger, M., Ziegler, S., Müller, U., Dobrozemsky, G., 2005. *In vitro* and *in vivo* evaluation of  $^{18}\text{F}$ -ciprofloxacin for the imaging of bacterial infections with PET. *Eur. J. Nucl. Med. Mol. Imaging* 32, 143–150.
- Larikka, M.J., Ahonen, A.K., Niemelä, O., Junila, J.A., Hämäläinen, M.M., Britton, K., 2002a.  $^{99\text{m}}\text{Tc}$ -ciprofloxacin (infection) imaging in the diagnosis of knee prosthesis infections. *Nucl. Med. Commun.* 23, 167–170.
- Larikka, M.J., Ahonen, A.K., Niemelä, O., Junila, J.A., Hämäläinen, M.M., Britton, K., 2002b. Comparison of  $^{99\text{m}}\text{Tc}$  ciprofloxacin,  $^{99\text{m}}\text{Tc}$  white blood cell and three-phase bone imaging in the diagnosis of hip prosthesis infections: improved diagnostic accuracy with extended imaging time. *Nucl. Med. Commun.* 23, 655–661.
- Lucignani, G., 2007. The many roads to infection imaging. *Eur. J. Nucl. Med. Mol. Imaging* 34, 1873–1877.
- Lupetti, A., Welling, M.M., Pauwels, E.K., Nibbering, P.H., 2007. Radiolabeled antimicrobial peptides for infection detection. *Lancet Infect. Dis.* 3, 223–239.
- Martin-Comin, J., Soroa, V., Rabiller, G., Galli, R., Cuesta, L., Roca, M., 2004. Diagnosis of bone infection with  $^{99\text{m}}\text{Tc}$ -ceftizoxime. *Rev. Esp. Med. Nucl.* 23, 357.
- Mostafa, M., Motaleb, M.A., Sakr, T.M., 2010. Labeling of ceftriaxone for infective inflammation imaging using  $^{99\text{m}}\text{Tc}$  eluted from  $^{99}\text{Mo}/^{99\text{m}}\text{Tc}$  generator based on zirconium molybdate. *Appl. Radiat. Isot.* 68, 1959–1963.
- Motaleb, M.A., 2007. Preparation and biodistribution of  $^{99\text{m}}\text{Tc}$ -lomefloxacin and  $^{99\text{m}}\text{Tc}$ -ofloxacin complexes. *J. Radioanal. Nucl. Chem.* 272, 95–99.
- Moustapha, M.E., Motaleb, M.A., Ibrahim, I.T., 2011. Synthesis of  $^{99\text{m}}\text{Tc}$ -oxybutynin for M3-receptor-mediated imaging of urinary bladder. *J. Radioanal. Nucl. Chem.* 287, 35–40.
- Moustapha, M.E., Motaleb, M.A., Ibrahim, I.T., Moustafa, M.E., 2013. Oxidative radioiodination of aripiprazole by chloramine-T as a route to a potential brain imaging agent: a mechanistic approach. *Radiochemistry* 55, 116–122.
- Nieto, M.J., Alovero, F.L., Manzo, R.H., Mazzieri, M.R., 2005. Benzenesulfonamide analogs of fluoroquinolones. Antibacterial activity and QSAR studies. *Eur. J. Med. Chem.* 40, 361–369.
- Oyen, W.J.G., Boerman, O.C., Corstens, F.H.M., 2001. Animal models of infection and inflammation. *J. Microbiol. Meth.* 47, 151–157.
- Palestro, C.J., 2007. *In vivo* leukocyte labeling. The quest continues. *J. Nucl. Med.* 48, 332–334.
- Pauwels, E.K., Welling, M.M., Lupetti, A., Nibbering, P.H., 2001. Concerns about  $^{99\text{m}}\text{Tc}$  labelled ciprofloxacin for infection detection—reply. *Eur. J. Nucl. Med.* 28, 781.
- Qaiser, S.S., Khan, A.U., Khan, M.R., 2010. Synthesis, biodistribution and evaluation of  $^{99\text{m}}\text{Tc}$ -sitaifloxacin kit: a novel infection imaging agent. *J. Radioanal. Nucl. Chem.* 284, 189–193.
- Rien, H.S., Huub, J.R., Otto, C.B., Rudi, D., Guido, S., 2004. Synthesis and comparison, of  $^{99\text{m}}\text{Tc}$ -enrofloxacin and  $^{99\text{m}}\text{Tc}$ -ciprofloxacin. *J. Nucl. Med.* 45, 2088–2094.
- Saha, G.B., 2004. *The Fundamentals of Nuclear Pharmacy*, fifth ed. Springer, New York.
- Sakr, T.M., Moustapha, M.E., Motaleb, M.A., 2013.  $^{99\text{m}}\text{Tc}$ -nebevivolol as a novel heart imaging radiopharmaceutical for myocardial infarction assessment. *J. Radioanal. Nucl. Chem.* 295, 1511–1516.
- Sarda, L., Saleh-Mghir, A., Peker, C., Meulemans, A., Crémieux, A.C., Guludec, L.D., 2002. Evaluation of (99m)Tc-ciprofloxacin scintigraphy in a rabbit model of Staphylococcus aureus prosthetic joint infection. *J. Nucl. Med.* 43, 239–245.
- Sarda, L., Crémieux, A., Lebellec, Y., Meulemans, A., Lebtahi, R., Hayem, G., 2003. Inability of  $^{99\text{m}}\text{Tc}$ -ciprofloxacin scintigraphy to discriminate between septic and sterile osteoarticular diseases. *J. Nucl. Med.* 44, 920–926.
- Siaens, R.H., Rennen, H.J., Boerman, O.C., Dierckx, R., Slegers, G., 2004. Synthesis and comparison of  $^{99\text{m}}\text{Tc}$ -enrofloxacin and  $^{99\text{m}}\text{Tc}$ -ciprofloxacin. *J. Nucl. Med.* 45, 2088–2094.
- Signore, A., Alessandria D, C., Lazzeri, E., Dierck, R., 2008. Can we produce an image of bacteria with radiopharmaceuticals? *Eur. J. Nucl. Med. Mol. Imaging* 35, 1051–1055.
- Singh, A.K., Verma, J., Bhatnagar, A., Ali, A., 2003. Tc-99m-labelled sparfloxacin: a specific infection imaging agent. *World J. Nucl. Med.* 2, 103–109.
- Singh, B., Babbar, A.K., Sarika, S., Kaul, A., Bhattacharya, A., Mittal, B.R., 2010. To evaluate the clinical efficacy of a single vial kit preparation of  $^{99\text{m}}\text{Tc}$ -ceftriaxone (Scintibact) for the diagnosis of orthopedic infections—first results. *J. Nucl. Med.* 51 (Suppl 2), 373.
- Starovoitova, V.N., Tchelidze, Lali, Wells, D.P., 2014. Production of medical radioisotopes with linear accelerators. *Appl. Radiat. Isot.* 85, 39–44.
- USP/NF, 2008. *United States Pharmacopeia/National Formulary*. US Pharmacopeia, USA.
- Yapar, A.F., Togrul, E., Kayaselcuk, U., 2001. The efficacy of technetium-99m ciprofloxacin imaging in suspected orthopedic infection: a comparison with sequential bone/gallium imaging. *Eur. J. Nucl. Med.* 28, 822–830.
- Ziessman, H.A., O'Malley, J.P., Thrall, J.H., 2014. *Nuclear Medicine*, fourth ed. Elsevier, USA, pp. 322–349.
- Zolle, I., 2007. *Technetium-99m Radiopharmaceuticals: Preparation and Quality Control in Nuclear Medicine*. Springer, Berlin.